Journal of Fluorescence (2019) 29:221–229
https://doi.org/10.1007/s10895-018-2331-3

ORIGINAL ARTICLE

Nitrogen-Doped Durian Shell Derived Carbon Dots for Inner Filter Effect Mediated Sensing of Tetracycline and Fluorescent Ink

Supuli Jayaweera[1,2] · Ke Yin[3] · Wun Jern Ng[4]

Received: 5 October 2018 / Accepted: 10 December 2018 / Published online: 19 December 2018

Abstract

Photoluminescent carbon dots have gained increasing attention in recent years due to their unique optical properties. Herein, a facile one-pot hydrothermal process is used to develop nitrogen-doped carbon dots (NCDs) with durian shell waste as the precursor and Tris base as the doping agent. The synthesized NCDs showed a quantum yield of 12.93% with a blue fluorescence under UV-light irradiation and maximum emission at 414 nm at an excitation wavelength of 340 nm. X-ray photoelectron spectroscopy (XPS) and Fourier transform infrared (FTIR) spectroscopy showed the presence of nitrogen and oxygen functional groups on the NCD surface. The particles were quasi-spherical with an average particle diameter of 6.5 nm. The synthesized NCDs were resistant to photobleaching and stable under a wide range of pH but were negatively affected by increasing temperature. NCDs showed high selectivity to Tetracycline as the fluorescence of NCDs was quenched significantly by Tetracycline as a result of the inner filter effect. Based on sensitivity experiments, a linear relationship ($R^2 = 0.989$) was developed over a concentration range of 0–30 μM with a detection limit of 75 nM ($S/N = 3$). The linear model was validated with two water samples (lake water and tap water) with relative recoveries of 98.6–108.5% and an RSD of <3.5%.

Keywords Carbon dots · Durian shell waste · Nitrogen doping · Fluorescent ink · Tetracycline detection

Introduction

In the past decade, carbon dots (CDs) have emerged as a novel class of nanomaterials that can be developed through economical and eco-friendly avenues using biomass resources [1–4]. This has resulted in CDs potentially having a significant role in the fabrication of sustainable materials. In addition, CDs also provide unique optical and electronic properties including tunable photoluminescence, low photobleaching, aqueous solubility, biocompatibility, and low toxicity [5]. These characteristics have resulted in CDs with diverse applications in the field of novel sensors for the detection of metal ions [1, 2, 5, 6] and organic compounds [7–9]. Apart from these pollutants, CDs can be effectively used as a fluorescent probe for emerging pollutants like antibiotics [10, 11]. With the ever-increasing global antibacterial market, overuse and misuse of antibiotics have led to the dissemination of antibiotic-resistant bacteria which is considered to be a major global health crisis [12]. Thus, there are increasing demands on developments in analytical techniques for antibiotic screening and detection. The current analytical practices involve high-performance liquid chromatography (HPLC) or mass spectroscopy (MS), capillary electrophoresis and iodometry, albeit these techniques have the downside of using expensive equipments and analytical columns, specialized manpower, chemical consumption and high maintenance cost [13]. Thus, developments of novel methods and sensors that are cheaper, faster and greener are important in future efforts of determination of antibiotics.

Durian (*Durio zibethinus*) is a tropical seasonal fruit that is popular in Asian countries including Thailand, Malaysia,

✉ Wun Jern Ng
WJNg@ntu.edu.sg

1 Nanyang Environment & Water Research Institute and Interdisciplinary Graduate School, Nanyang Technological University, Singapore, Singapore

2 Residues & Resource Reclamation Centre, Nanyang Environment & Water Research Institute, Nanyang Technological University, Singapore, Singapore

3 Department of Environmental Engineering, School of Biology and the Environment, Nanjing Forestry University, Nanjing, Jiangsu, China

4 Environmental Bio-innovations Group (EBiG), School of Civil and Environmental Engineering, Nanyang Technological University, Singapore, Singapore

Indonesia, China, Singapore and Taiwan with an annual harvest of 1.4 million tons [14]. The issue with durian is 60–75% (*w*/w) of the entire fruit is thrown away as waste, mainly in the form of its shell [15]. The bulk of durian shell waste is cellulose (~60%), but it also contains extractives which can be a rich source of carboxylic acids and phenolic groups [16, 17]. During hydrothermal carbonisation, the lignocellulosic biomass will hydrolyze, forming oligomers and glucose [18]. These intermediary products will further undergo complex pathways involving dehydration, condensation, polymerization and a nucleation reaction to form a crystalline nanoparticle core with a hydrophilic shell containing oxygen functional groups [18–20]. Oxygen-rich functional groups including -COOH and -OH are expected to provide versatile anchoring points for doping agents to improve the performance of carbon dots [17, 21]. Thus, elemental doping with nitrogen is proposed where the nitrogen containing chromophore can act as a surface passivation agent to improve the quantum yield of the synthesized CDs [22]. In this paper, nitrogen doped florescent CDs (NCDs) are produced from Durian Shell Waste (DSW) with Tris base as the doping agent in a one-pot HTC process. The NCDs are characterised for physical, chemical and optical properties. Further, the synthesized NCDs have been tested for selective and sensitive detection of Tetracycline (TC). TC is a broad spectrum antibacterial widely used as a first-line antibiotic in human and veterinary medicine [23]. In recent years, several works have been published in association with tetracycline detection. However, most of these reports include either a complex synthetic process or expensive chemicals. This paper identifies the potential of using a waste material with naturally existing oxygen functional groups to produce a Tetracycline sensor that shows better or comparable sensing results to these previous reports. The proposed sensing methodology is further validated with two real water systems. This paper introduces a fast, sensitive and straightforward fluorescent probe to detect TC in an aqueous medium and an efficient fluorescent ink.

Experimental

Materials and Chemicals

Durian shell was obtained from the local markets in Singapore. Tris base was obtained from Promega Corporation (U.S.). Amoxicillin sodium was purchased from MedChemExpress. (U.S.). Quinine sulfate was purchased from Alfa Aesar. (U.S.). Dichloromethane, Streptomycin sulfate, Ampicillin sodium, Chloramphenicol, Lincomycin hydrochloride, Tetracycline hydrochloride and sulfanilamide were obtained from Sigma-Aldrich Co. LLC. (U.S.). NaOH was obtained from Merck Pte. Ltd. (U.S.). All chemicals were of analytical grade and used as received.

Sample Preparation

Durian shells were washed thoroughly with tap water and cut into 1–2 cm pieces and dried at 105 °C for 24 h. The dried durian pieces were ground with a ball mill (RETSCH PM 100, Germany) and sieved with a 0.22 mm wire mesh. The powdered DSW was stored at 4 °C until use.

Synthesis of C-Dots

The NCDs were synthesized by hydrothermal carbonisation of DSW as shown in Fig. 1. 1 g of powdered DSW with 0.4 g of Tris base was introduced to 25 ml of DI water. The mixture was transferred to a Teflon-lined autoclave and heated at 210 °C for 12 h. The resulting NCD solution was then allowed to cool naturally to room temperature and then filtered with a 0.45 μm filter followed with 0.22 μm filter membranes to remove the larger particles. The solution was then washed with dichloromethane to remove any unreacted organic moieties and subjected to dialysis against deionized (DI) water through a dialysis membrane (3500 MWCO) for 48 h before use. The produced NCD solution was stored at 4 °C until characterisation.

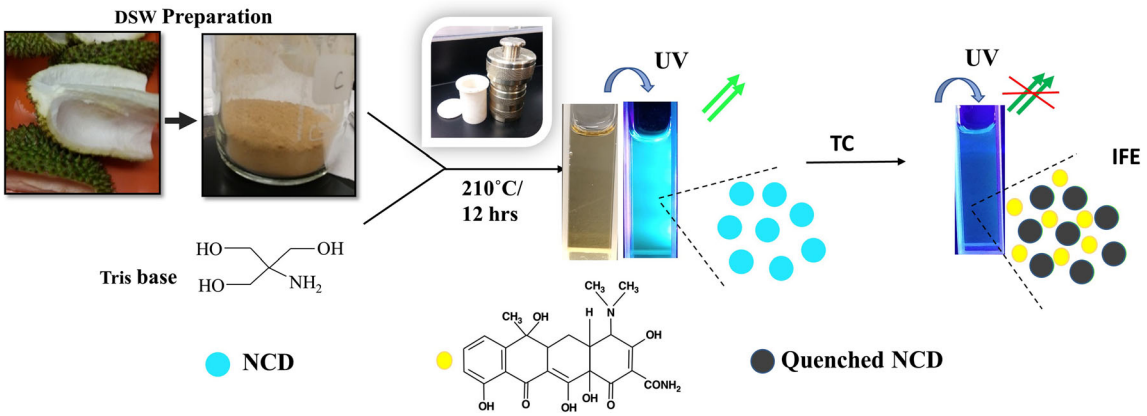

Fig. 1 Schematic diagram of the preparation and application of NCDs

Characterisation

Fluorescence spectra were acquired with the Agilent Cary Eclipse Fluorescence Spectrophotometer (USA). Ultraviolet-Visible absorption spectra were recorded with a Varian Cary 50 UV/Vis Spectrophotometer (USA). Time resolved fluorescence spectroscopy was done with Horiba fluorolog-3 spectrofluorometer (Japan) equipped with a 360 nm nanoLED. Fourier transform infrared spectroscopy (FTIR) was measured with a Bruker Tensor 27 FTIR spectrophotometer (USA). Transmission electron microscopy (TEM) was performed on a JEOL 2010 HR transmission electron microscope (Japan). Raman pattern was obtained with the HORIBA XploRAPLUS Raman Microscope (Japan). X-ray photoelectron spectroscopy (XPS) measurements were conducted on a Kratos Analytical AXIS Supra photoelectron spectrometer (UK). X-ray Powder Diffraction (XRD) was performed on a Bruker D8 Advance (USA).

Quantum Yield (QY) Measurement

The fluorescence quantum yield of NCDs was determined using quinine sulfate (QY is 54% in 0.5 M H_2SO_4 solution) as a standard sample at 366 nm excitation wavelength and calculated with the following equation [24]

$$Q_{CD} = Q_{st}\left(\frac{I_{NCD}}{I_{st}}\right)\left(\frac{A_{st}}{A_{CD}}\right)\left(\frac{\eta_{CD}}{\eta_{st}}\right)^2$$

where subscripts "NCD" and "st" stands for NCDs and reference standard respectively. "Q" refers to the QY, "I" refers to the integrated Photoluminescence (PL) intensity, "A" refers the absorbance measured at the excited wavelength and "η" refers to the refractive index. To minimize re-absorption effects in the 10 mm fluorescence cuvette, absorbencies were kept under 0.1. QY of the NCDs was calculated to be 12.93%.

Fluorescence Measurement

To assess the selectivity of antibiotics, Amoxicillin, Streptomycin, Chloramphenicol, Sulfanilamide, Lincomycin, Tetracycline (TC) and Ampicillin were evaluated with the NCDs. In a typical 2 ml volume assay, final NCD concentration was maintained at 125 μg/ml while the antibiotic concentration was 100 μM. The PL spectrum was recorded at an excitation wavelength of 340 nm. The emission was recorded from 350 nm to 600 nm. Detector voltage was maintained at 800 V throughout the samples and all measurements were performed in triplicates. Then, to determine the sensitivity, different concentrations of TC solutions from 2 μM–100 μM were prepared. The NCD concentration was maintained at 125 μg/ml. All solutions were prepared in DI water.

Two different water samples (Jurong Lake water and tap water) were used to validate the proposed TC sensor. All water samples were filtered with 0.22 μm syringe filter membranes to remove particles. Subsequently, 2 ml of the real water samples were spiked with known concentrations of TC and exposed to 125 μg/ml NCD. The fluorescence emission spectra were analyzed at an excitation wavelength of 340 nm.

Results and Discussion

Characterisation of NCD

Characterisation tests were conducted to get insights into the PL mechanism of the NCDs. The functional groups of the synthesized NCDs were evaluated by the FTIR spectrum (Fig. 2a). The broad absorption peak at 3413 cm^{-1} and 3243 cm^{-1} corresponds to the N-H and phenolic-OH, and stretching vibrations [2]. The absorption peak at 2916 cm^{-1} and 2815 cm^{-1} were assigned to the C-H stretching vibrations [5, 25]. The absorption at 1750 cm^{-1} and 1650 cm^{-1} corresponds with -CO- (carboxylic acid) and C=N functional groups, respectively [2]. The aromatic C = C bending at 1604 cm^{-1} indicates the presence of a sp2 hybridized honeycomb lattice. The band at 1200 cm^{-1} represents the C-O-C group [25] while the stretching vibration bands at 1090 cm^{-1} indicates -C-O oxygen containing functional groups including carboxyl groups [5]. Overall, the presence of these oxygen and nitrogen containing functional groups improve the dispersibility of NCDs in water by enhancing the hydrophilicity [26].

Raman spectroscopy (Fig. 2b) indicated two vibrational peaks, at 1380 and 1607 cm^{-1}, which corresponded with disordered (D) structures in graphene and graphitic (G) bands respectively [27]. The ratio of D and G peak intensities (I_D/I_G) was around 1.42, which suggested the NCDs produced had high surface defects compared to the sp2 graphitic structure. Further, the XRD patterns were used to confirm the crystalline phase of the synthesized NCDs as shown in Fig. 2c. The peak at 16° showed the presence of disordered carbon [28] and the broad diffraction peak around 22° which corresponded with a carbon lattice spacing of 3.99 Å was slightly higher than the (002) lattice spacing of 3.44 Å [25]. This increment was attributed to the increase in the amorphous nature of the NCD surface [29].

TEM imaging was employed to view the particle morphology and size distribution of the NCDs. Results indicated the NCDs were well dispersed (Fig. 2d), and shape of the NCDs was quasi-spherical. The average diameter of the particles was measured to be 6.5 nm (Fig. 2e).

Figure 3a represents the XPS survey spectrum conducted for C, O, N elements on the NCDs. The corresponding *w*/w elemental composition were 75.32%, 22.35% and 2.33%, respectively. The high resolution C1S spectrum shown by

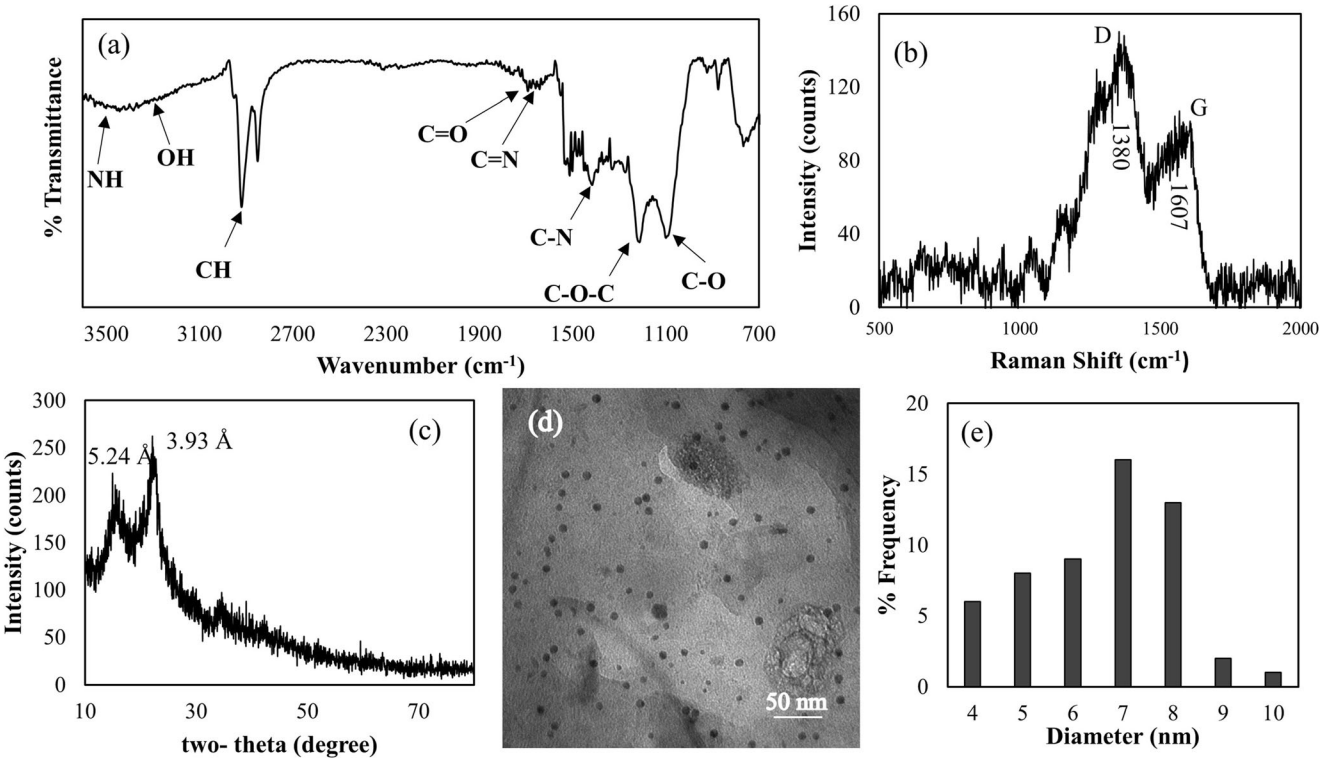

Fig. 2 **a** FTIR Spectra, **b** Raman Spectra, **c** XRD Spectra, **d** TEM images of the NCDs, **e** particle diameter distribution

Fig. 3b is deconvoluted into three peaks at 284.8, 286.5 and 288.3 eV, which is attributed to C-C/C=C, C-O and C=O bonds, respectively [30, 31]. The O1s spectrum (Fig. 3c) was resolved to two peaks at 531.7 and 532.9 eV, which are due to C-O and C − OH/C − O − C groups, respectively [5]. The N1 s spectrum (Fig. 3d) was deconvoluted to three peaks at 397.5 ev for C ≡ N, 399.7 eV for C-N and 400.9 eV for N-H bonds [5, 32]. Thus, XPS results further confirmed the presence of oxygen and nitrogen functional groups on the synthesized NCDs.

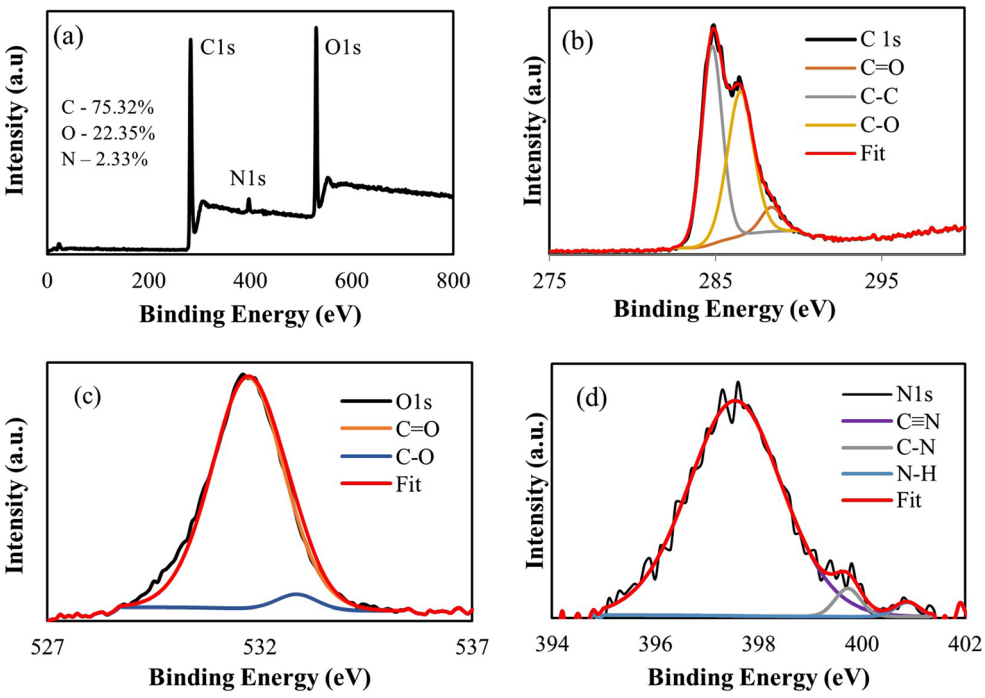

Fig. 3 **a** XPS spectrum of the NCDs, **b**, **c**, and **d** High-resolution C1s, O1s, and N1 s XPS spectra of the NCDs

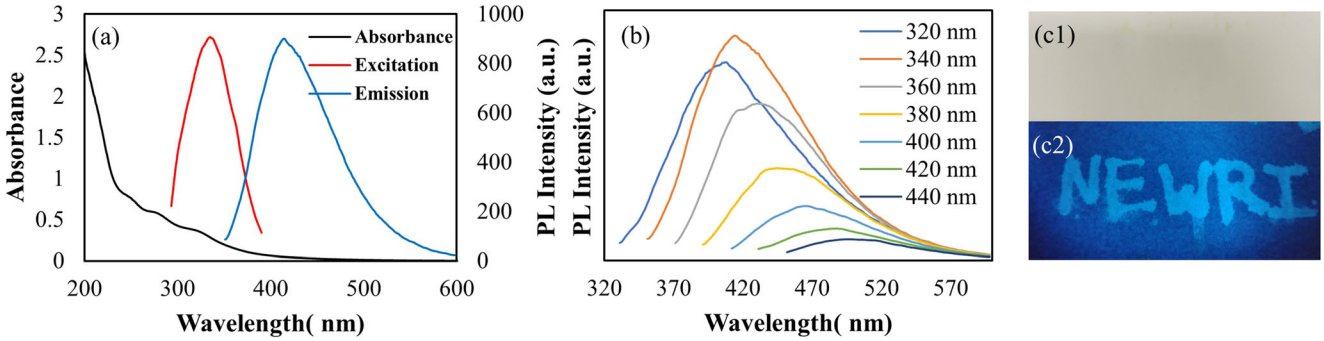

Fig. 4 The optical properties of the NCDs. **a** UV/Vis absorption spectrum with maximum emission and excitation spectra, **b** PL emission spectra of NCDs at different excitation wavelengths and Photographic image of a text written fluorescent ink under (**c1**) normal indoor light and (**c2**) UV-light

Figure 4a illustrates the UV/vis absorption spectrum of NCDs with the maximum excitation and emission spectra. UV-absorption of the NCDs (Fig. 4a) conformed with the general optical absorption of the carbon quantum dots in the UV region with a tail extending to the visible range [33–35]. However, absorption shoulders could be observed at 254, 280 and 320 nm. The broad peak at 254 and 280 nm was attributed to π -π* aromatic sp2 hybridisation [36, 37] while the 320 nm peak corresponded with the n– π* transition of the carbonyl group [38]. The maximum photoluminescence was observed at 414 nm upon excitation at 340 nm. Figure 1 shows the synthesized NCD solution exhibited a bright blue colour under a UV light of 365 nm which was transparent yellow under daylight. The synthesized NCDs exhibited excitation dependent emission between 320 and 440 nm which is shown in Fig. 4b, and this was attributed to the presence of trap states arising from the surface defects [39, 40]. The NCD solution was used as a fluorescent ink directly without any pretreatment as shown in Fig. 4c. The photographs show the text was distinct from the background under UV light and so suggested the NCDs can be material for fluorescent ink.

To investigate the applicability of the synthesized NCDs as a fluorescent probe, the stability of the NCDs dispersed in water was evaluated by measuring the PL intensity variation with pH, temperature, and time. Under varying pH values from 3 to 11 (Fig. 5a), the PL intensity was consistent with two drops at pH 5 and pH 10. This is due to the N-H and COO- groups present on the NCD surface which created varying isoelectric points and dissociation constants [41]. However, the overall intensity variation was within a relative standard deviation (RSD) of 2.1%. Thus, it can be considered the NCDs were resistant to pH variation. In contrast, the intensity variation with temperature was significant where lower temperatures had higher fluorescent intensity (Fig. 5b). The temperature dependent fluorescence was attributed to thermal activation of non-radiative trappings in surface and defective sites [42]. The photostability of NCDs was also quantified by continuous exposure to UV irradiation (Fig. 5c) and the intensity was preserved at 97% of its initial value after continuous exposure to UV irradiation by 18 W Hg lamp for 120 mins, suggesting the high photostability of the synthesized NCDs.

Mechanism and Detection of Antibiotics

To investigate the influence of antibiotics to the photoluminescence property of NCDs, First, the selectivity towards different antibiotics including Lincomycin (Lin), Tetracycline, Amoxicillin (Amox), Ampicillin (Amp), Streptomycin (Str), Sulfanilamide (Sulf) and Chloramphenicol (Chlo) was investigated (Fig. 6a) and the results indicated that

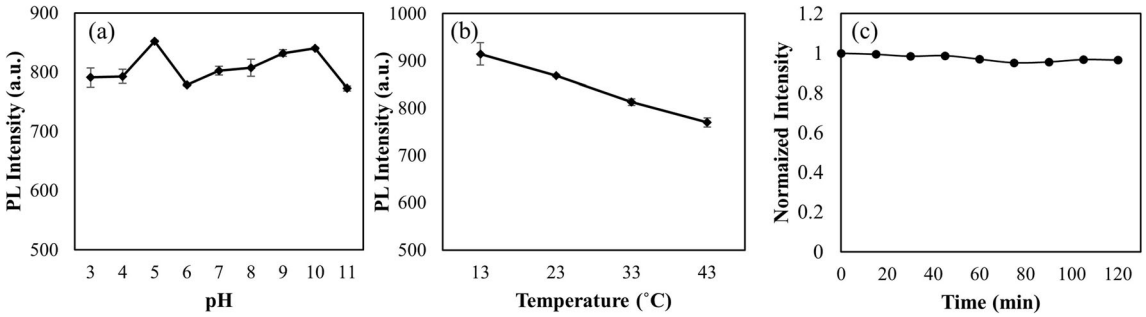

Fig. 5 The PL variation of NCDs with **a** solution pH, **b** solution temperature and **c** the effect of time measured by a continuous exposure to UV irradiation by a Hg lamp

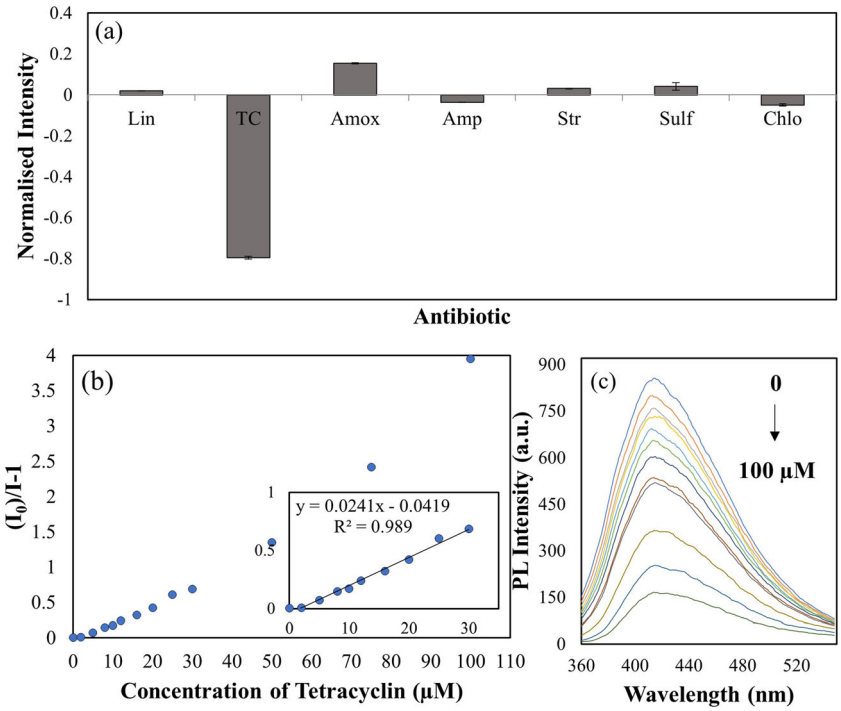

Fig. 6 **a** Selectivity of NCDs towards different antibiotics, **b** Fluorescent intensity with TC concentration **c** PL emission spectra with increasing TC

NCDs had strong sensitivity towards TC with a fluorescent quenching around 80% and moderately sensitive towards Amoxicillin with fluorescent enhancement around 16% at an antibiotic concentration of 100 μM. The sensitivity of NCDs fluorescence quenching to TC was further evaluated with various concentrations of TC. The fluorescence intensity declined gradually with the increase of TC concentrations ranging from 0 to 100 μM (Fig. 6b and c). A good linear regression correlation was found as below:

$$Y = 0.0241\,X - 0.419$$

with a correlation coefficient R^2 of 0.989 over the concentration range 0–30 μM. The lowest detection limit (LOD) was calculated to be 75 nM based on a signal to noise ratio of 3 and as seen on Table 1, the performance of TC sensing was better or comparable with previously reported fluorescent probes.

To explore the sensing mechanism of TC, a series of studies were carried out. According to Fig. 7a, there is a good spectral overlap of the absorption spectrum of TC with the excitation spectra of the NCDs compared to other antibiotics. This indicated the quenching could happen by inner filter effect (IFE) or/and fluorescence resonance energy transfer (FRET) process. However, the lifetime of the NCDs in the presence and absence of TC remained unchanged (Fig. 7b) and was measured to be at 5.8 ns. Thus, it was reasonable to exclude FRET as a possible mechanism in TC quenching. Further, the absorption spectra of the NCDs, NCDs with TC and TC were examined (Fig. 7c) and there was no difference in the NCD absorption spectra when TC was added. This confirmed the

Table 1 Comparison of TC detection with other reported probes in recent years

Fluorescent probe	Linear range (μM)	LOD (nM)	Reference
Europium-doped CDs	0.5–200	300	[43]
Citric acid and glutathione CDs	2–150	520	[44]
Polymer imprinted CDs	0.02–40	5.48	[45]
Silica imprinted CDs	0.1–50	9.0	[46]
Cadmium telluride quantum dots	13.4–134	308	[47]
Molecularly imprinted polymer ZnO nanorods	2–120	127	[48]
Nitrogen doped Durian shell waste CDs	0–30	75	This work

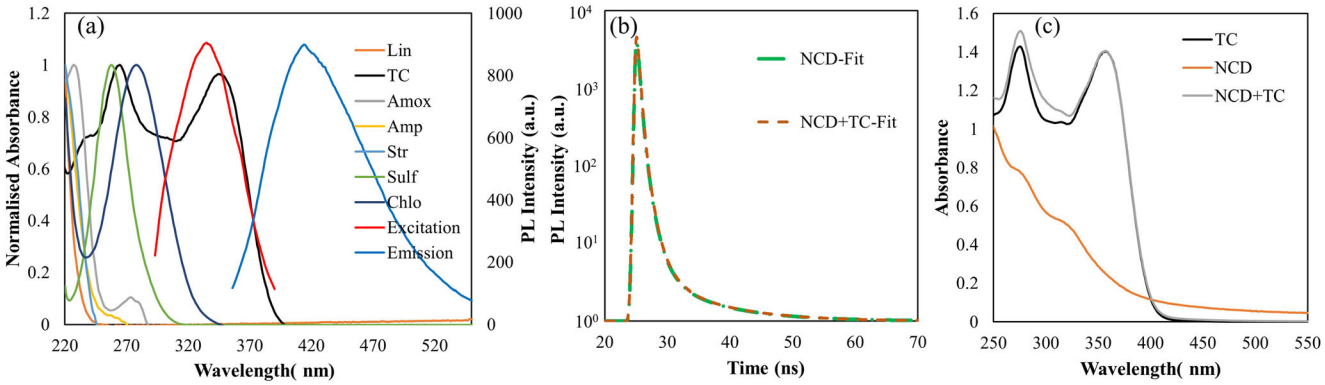

Fig. 7 **a** Normalised UV-Vis adsorption of antibiotics with excitation and emission spectra of NCDs, **b** Time-correlated single-photon counting (TCSPC) of NCDs in the presence and absence of TC and **c** UV-Vis adsorption for TC, NCDs and NCDs with TC

absence of ground state complex formation. Thus, the IFE served as the primary quenching mechanism for NCDs in the presence of TC. In recent years, IFE based sensors have gained more attention due to their simplicity and flexibility as these have no requirement for electron or energy transfer processes or any covalent linking between the fluorophore and quencher [44]. Thus, the synthesized NCDs provided a highly selective, sensitive and simpler sensing platform to detect TC.

To validate the sensing parameters of TC with NCDs, experiments were conducted on actual water samples. The water samples were spiked with known concentrations of TC and the recovery percentages and relative standard deviations (RSD) are as shown in Table 2.

As expected the fluorescence decreased with increasing TC concentration and the recoveries were between 98.6–108.5% while the RSD was below 3.5%. This reinforced the argument NCDs is a promising sensor to detect TC in environmental water samples.

Conclusion

Blue-emitting nitrogen doped NCDs could be successfully synthesized using a one-pot hydrothermal method using durian shell waste with tris base as the doping agent. The presence of natural existing oxygen groups in the durian shell provided versatile anchoring points for the nitrogen dopant which resulted in carbon dots with good fluorescent properties and stability. Thus, durian shells can possibly be an effective and cheap carbon precursor material for future CD development. The synthesized NCDs exhibited high selectivity towards TC based on the IFE process with a limit of detection at 75 nM. The IFE based sensing strategy would provide an efficient, convenient and sensitive technique to detect TC while avoiding any complex covalent bonding. Thus, the synthesized NCDs have a high potential for use as an efficient and simple TC detection sensor in environmental systems.

Table 2 Detection of TC in actual water samples ($n = 3$)

Sample	Spiked concentration (μM)	Measured concentration (μM)	Recovery %	RSD %
Lake water	5.00	5.04	100.86	3.42
	10.00	10.85	108.46	2.52
	20.00	20.91	104.54	0.69
Tap water	5.00	5.31	106.28	0.92
	10.00	10.51	105.11	0.79
	20.00	19.72	98.62	1.56

Acknowledgments The authors would like to thank Interdisciplinary Graduate school of Nanyang Technological University and Nanyang Environment & Water Research Institute for the financial support extended to this study. We would like to acknowledge the Facility for Analysis, Characterization, Testing and Simulation, Nanyang Technological University, Singapore, for use of their transmission electron microscopy facilities.

Compliance with Ethical Standards

Conflicts of Interest None.

Publisher's Note Springer Nature remains neutral with regard to jurisdictional claims in published maps and institutional affiliations.

References

1. Rooj B, Dutta A, Islam S, Mandal U (2018) Green synthesized carbon quantum dots from Polianthes tuberose L. petals for copper (II) and iron (II) detection. J Fluoresc 28(5):1261–1267
2. Shen J, Shang S, Chen X, Wang D, Cai Y (2017) Highly fluorescent N, S-co-doped carbon dots and their potential applications as antioxidants and sensitive probes for Cr (VI) detection. Sensors Actuators B Chem 248:92–100
3. Liu X-J, Guo M-L, Yin X-Y, Huang J (2013) A simple route to prepare carbonaceous nanospheres from bagasse. Mater Lett 106:30–32

4. Gedda G, Lee C-Y, Lin Y-C, Wu H-f (2016) Green synthesis of carbon dots from prawn shells for highly selective and sensitive detection of copper ions. Sensors Actuators B Chem 224:396–403
5. Shi J, Ni G, Tu J, Jin X, Peng J (2017) Green synthesis of fluorescent carbon dots for sensitive detection of Fe 2+ and hydrogen peroxide. J Nanopart Res 19(6):209
6. Chang MMF, Ginjom IR, Ngu-Schwemlein M, Ng SM (2016) Synthesis of yellow fluorescent carbon dots and their application to the determination of chromium (III) with selectivity improved by pH tuning. Microchim Acta 183(6):1899–1907
7. Shi Y, Pan Y, Zhang H, Zhang Z, Li M-J, Yi C, Yang M (2014) A dual-mode nanosensor based on carbon quantum dots and gold nanoparticles for discriminative detection of glutathione in human plasma. Biosens Bioelectron 56:39–45
8. Dai H, Shi Y, Wang Y, Sun Y, Hu J, Ni P, Li Z (2014) A carbon dot based biosensor for melamine detection by fluorescence resonance energy transfer. Sensors Actuators B Chem 202:201–208
9. Bharathi D, Siddlingeshwar B, Krishna RH, Singh V, Kottam N, Divakar DD, Alkheraif AA (2018) Green and cost effective synthesis of fluorescent carbon quantum dots for dopamine detection. J Fluoresc 28(2):573–579
10. Hua J, Jiao Y, Wang M, Yang Y (2018) Determination of norfloxacin or ciprofloxacin by carbon dots fluorescence enhancement using magnetic nanoparticles as adsorbent. Microchim Acta 185(2):137
11. Niu J, Gao H (2014) Synthesis and drug detection performance of nitrogen-doped carbon dots. J Lumin 149:159–162
12. Gullberg E, Cao S, Berg OG, Ilbäck C, Sandegren L, Hughes D, Andersson DI (2011) Selection of resistant bacteria at very low antibiotic concentrations. PLoS Pathog 7(7):e1002158
13. de Marco BA, Natori JSH, Fanelli S, Tótoli EG, Salgado HRN (2017) Characteristics, properties and analytical methods of amoxicillin: a review with green approach. Crit Rev Anal Chem 47(3): 267–277
14. Foo K, Hameed B (2011) Transformation of durian biomass into a highly valuable end commodity: trends and opportunities. Biomass Bioenergy 35(7):2470–2478
15. Foo K, Hameed B (2012) Textural porosity, surface chemistry and adsorptive properties of durian shell derived activated carbon prepared by microwave assisted NaOH activation. Chem Eng J 187: 53–62
16. Tan Y, Abdullah A, Hameed B (2017) Fast pyrolysis of durian (Durio zibethinus L) shell in a drop-type fixed bed reactor: pyrolysis behavior and product analyses. Bioresour Technol 243:85–92
17. Jayaweera S, Yin K, Hu X, Ng WJ (2018) Facile preparation of fluorescent carbon dots for label-free detection of Fe3+. J Photochem Photobiol A Chem 370:156–163
18. Wang T, Zhai Y, Zhu Y, Li C, Zeng G (2018) A review of the hydrothermal carbonization of biomass waste for hydrochar formation: process conditions, fundamentals, and physicochemical properties. Renew Sust Energ Rev 90:223–247
19. Jelinek R (2017) Carbon-dot synthesis. In: Carbon quantum dots synthesis, properties and applications (pp. 5–27). Springer International Publishing. https://doi.org/10.1007/978-3-319-43911-2
20. Sahu S, Behera B, Maiti TK, Mohapatra S (2012) Simple one-step synthesis of highly luminescent carbon dots from orange juice: application as excellent bio-imaging agents. Chem Commun 48(70):8835–8837
21. Loo AH, Sofer Z, Bouša D, Ulbrich P, Bonanni A, Pumera M (2016) Carboxylic carbon quantum dots as a fluorescent sensing platform for DNA detection. ACS Appl Mater Interfaces 8(3): 1951–1957
22. Wu ZL, Zhang P, Gao MX, Liu CF, Wang W, Leng F, Huang CZ (2013) One-pot hydrothermal synthesis of highly luminescent nitrogen-doped amphoteric carbon dots for bioimaging from Bombyx mori silk–natural proteins. J Mater Chem B 1(22): 2868–2873
23. Jalalian SH, Taghdisi SM, Danesh NM, Bakhtiari H, Lavaee P, Ramezani M, Abnous K (2015) Sensitive and fast detection of tetracycline using an aptasensor. Anal Methods 7(6):2523–2528
24. Brouwer AM (2011) Standards for photoluminescence quantum yield measurements in solution (IUPAC Technical Report). Pure Appl Chem 83(12):2213–2228
25. Adedokun O, Roy A, Awodugba AO, Devi PS (2017) Fluorescent carbon nanoparticles from Citrus sinensis as efficient sorbents for pollutant dyes. Luminescence 32(1):62–70
26. Hsu P-C, Chang H-T (2012) Synthesis of high-quality carbon nanodots from hydrophilic compounds: role of functional groups. Chem Commun 48(33):3984–3986
27. Edison TNJI, Atchudan R, Shim J-J, Kalimuthu S, Ahn B-C, Lee YR (2016) Turn-off fluorescence sensor for the detection of ferric ion in water using green synthesized N-doped carbon dots and its bio-imaging. J Photochem Photobiol B Biol 158:235–242
28. Xu H, Xie L, Hakkarainen M (2017) Coffee-ground-derived quantum dots for aqueous processable nanoporous graphene membranes. ACS Sustain Chem Eng 5(6):5360–5367
29. Mewada A, Pandey S, Shinde S, Mishra N, Oza G, Thakur M, Sharon M, Sharon M (2013) Green synthesis of biocompatible carbon dots using aqueous extract of Trapa bispinosa peel. Mater Sci Eng C 33(5):2914–2917
30. Ye Q, Yan F, Luo Y, Wang Y, Zhou X, Chen L (2017) Formation of N, S-codoped fluorescent carbon dots from biomass and their application for the selective detection of mercury and iron ion. Spectrochim Acta A Mol Biomol Spectrosc 173:854–862
31. Zhang H, Kang S, Wang G, Zhang Y, Zhao H (2016) Fluorescence determination of nitrite in water using prawn-shell derived nitrogen-doped carbon nanodots as fluorophores. ACS Sensors 1(7):875–881
32. Desimoni E, Brunetti B (2015) X-ray photoelectron spectroscopic characterization of chemically modified electrodes used as chemical sensors and biosensors: a review. Chemosensors 3(2):70–117
33. De B, Karak N (2013) A green and facile approach for the synthesis of water soluble fluorescent carbon dots from banana juice. RSC Adv 3(22):8286–8290
34. Wang Y, Hu A (2014) Carbon quantum dots: synthesis, properties and applications. J Mater Chem C 2(34):6921–6939
35. Zhang J-H, Niu A, Li J, Fu J-W, Xu Q, Pei D-S (2016) In vivo characterization of hair and skin derived carbon quantum dots with high quantum yield as long-term bioprobes in zebrafish. Sci Rep 6:37860
36. Yang R, Guo X, Jia L, Zhang Y, Zhao Z, Lonshakov F (2017) Green preparation of carbon dots with mangosteen pulp for the selective detection of Fe3+ ions and cell imaging. Appl Surf Sci 423:426–432
37. Li H, He X, Kang Z, Huang H, Liu Y, Liu J, Lian S, Tsang CHA, Yang X, Lee ST (2010) Water-soluble fluorescent carbon quantum dots and photocatalyst design. Angew Chem Int Ed 49(26):4430–4434
38. Meiling TT, Cywiński PJ, Bald I (2016) White carbon: fluorescent carbon nanoparticles with tunable quantum yield in a reproducible green synthesis. Sci Rep 6:28557
39. Su Z, Ye H, Xiong Z, Lou Q, Zhang Z, Tang F, Tang J, Dai J, Shan C, Xu S (2018) Understanding and manipulating luminescence in carbon nanodots. Carbon 126:58–64
40. Baker SN, Baker GA (2010) Luminescent carbon nanodots: emergent nanolights. Angew Chem Int Ed 49(38):6726–6744
41. Sun D, Ban R, Zhang P-H, Wu G-H, Zhang J-R, Zhu J-J (2013) Hair fiber as a precursor for synthesizing of sulfur-and nitrogen-co-doped carbon dots with tunable luminescence properties. Carbon 64:424–434

42. Yu P, Wen X, Toh Y-R, Tang J (2012) Temperature-dependent fluorescence in carbon dots. J Phys Chem C 116(48):25552–25557
43. Liu ML, Chen BB, Yang T, Wang J, Liu XD, Huang CZ (2017) One-pot carbonization synthesis of europium-doped carbon quantum dots for highly selective detection of tetracycline. Methods Appl Fluoresc 5(1):015003
44. Lin M, Zou HY, Yang T, Liu ZX, Liu H, Huang CZ (2016) An inner filter effect based sensor of tetracycline hydrochloride as developed by loading photoluminescent carbon nanodots in the electrospun nanofibers. Nanoscale 8(5):2999–3007
45. Hou J, Li H, Wang L, Zhang P, Zhou T, Ding H, Ding L (2016) Rapid microwave-assisted synthesis of molecularly imprinted polymers on carbon quantum dots for fluorescent sensing of tetracycline in milk. Talanta 146:34–40
46. Yang J, Lin Z-Z, Nur A-Z, Lu Y, Wu M-H, Zeng J, Chen X-M, Huang Z-Y (2018) Detection of trace tetracycline in fish via synchronous fluorescence quenching with carbon quantum dots coated with molecularly imprinted silica. Spectrochim Acta A Mol Biomol Spectrosc 190:450–456
47. Gao C, Liu Z, Chen J, Yan Z (2013) A novel fluorescent assay for oxytetracycline hydrochloride based on fluorescence quenching of water-soluble CdTe nanocrystals. Luminescence 28(3):378–383
48. Zhou Z, Lu K, Wei X, Hao T, Xu Y, Lv X, Zhang Y (2016) A mesoporous fluorescent sensor based on ZnO nanorods for the fluorescent detection and selective recognition of tetracycline. RSC Adv 6(75):71061–71069